


# Nanocomposite fibers of poly(lactic acid)/titanium dioxide prepared by solution blow spinning

Rodrigo G. F. Costa<sup>1</sup> · Glauca S. Brichi<sup>2</sup> ·  
Caue Ribeiro<sup>1</sup>  · Luiz H. C. Mattoso<sup>1</sup>

Received: 2 July 2015 / Revised: 21 February 2016 / Accepted: 8 March 2016 /  
Published online: 26 March 2016  
© Springer-Verlag Berlin Heidelberg 2016

**Abstract** Solution blow spinning (SBS) is a recent technology to produce polymer micro- and nanofibers, including nanocomposites loaded with a wide range of nanoparticles. Because of its novelty, various studies about the properties of the produced materials are necessary, especially those related to material stability. In the present study, poly(lactic acid) (PLA)/titanium dioxide anatase (TiO<sub>2</sub>) nanocomposite fibers, with different TiO<sub>2</sub> percentages, were produced by the SBS method. The spun nanocomposite fibers were characterized by scanning electron microscopy (SEM), transmission electron microscopy (TEM), X-ray diffraction, thermogravimetric analysis and differential scanning calorimetry (DSC). Moreover, the photocatalytic degradation of Rhodamine B (RhB) dye and PLA degradation by UV-C lamps were investigated. SEM and TEM micrographs show that the SBS method produced PLA/TiO<sub>2</sub> nanofibers with uniform morphology and without beads. The DSC analyses and X-ray diffraction patterns show that incorporation of TiO<sub>2</sub> nanoparticles could influence the PLA nanocomposite crystallinity. PLA photocatalytic degradation experiments demonstrate that the weight loss of the polymer increases with an increase in TiO<sub>2</sub> content. The present results indicate that the SBS method can be used to produce biodegradable nanocomposite fibers with good properties and potential applications.

**Keywords** Solution blow spinning · Nanofibers · Nanocomposite fibers · Poly(lactic acid) · Titanium dioxide nanoparticles

---

✉ Caue Ribeiro  
caue.ribeiro@embrapa.br

<sup>1</sup> Laboratório Nacional de Nanotecnologia para o Agronegócio, Embrapa Instrumentação, Rua XV de Novembro, 1452, Centro, São Carlos, SP 13.560-970, Brazil

<sup>2</sup> Departamento de Química, Universidade Federal de São Carlos, Rodovia Washington Luís, Monjolinho, São Carlos, SP 13.565-905, Brazil

## Introduction

Poly(lactic acid) (PLA) is a biodegradable and compostable polymer, whose monomer, L-lactic acid, can be obtained from renewable resources such as wheat, starch, and sugar beets [1, 2]. It has been explored in medical, packaging, and textile applications in different forms, such as nanoparticles and microparticles, films and fiber mats fabricated by electrospinning [1–4]. Polymer nanofibers have a larger surface-to-volume ratio, small pore size and better mechanical properties than other morphologies, which explains the increasing interest in techniques capable of producing such fibers in a reproducible manner [4–6]. Moreover, the nanofiber mats can be produced in almost any size and it is possible to tailor their porosity [4–6]. Because of these properties, they have been used in several fields, such as sensors, biomedical devices, drug delivery systems, and nanocomposites [7–10].

Among the most interesting materials for tailoring functional nanocomposites, titanium dioxide ( $\text{TiO}_2$ ) nanoparticles are very attractive because of their chemical stability, photocatalytic activity, and UV absorbance [11–13]. This material has been investigated as a filler for polymers in nanocomposites, such as poly( $\epsilon$ -caprolactone) (PCL), poly(acrylonitrile) (PAN), poly(ethylene terephthalate) (PET), and poly(lactic acid) (PLA) [14–19]. Moreover, the electrospinning technique has been used to prepare nanocomposite fibers loaded with  $\text{TiO}_2$  nanoparticles, with high surface-area and porosity, such as PVA/ $\text{TiO}_2$ , PLA/ $\text{TiO}_2$ , etc. [12–20] The PLA/ $\text{TiO}_2$  system was investigated by different methods [1, 2, 18] such as spin coating (thin film) and extrusion–injection processing (thick film) [1], solution casting [2], and solution blending [18]. However, few studies have investigated the incorporation of  $\text{TiO}_2$  by spinning techniques, despite reports about the potential application of electrospun PLA/ $\text{TiO}_2$  fibers as drug carriers, because of the good biocompatibility and large surface area of the nanocomposites [20].

Solution blow spinning (SBS) was discovered recently as a new and versatile method to produce fibers from polymer solutions with small diameters, ranging from a few tens of nanometers to several micrometers [4, 7–9]. The SBS method uses conceptual elements of melt blowing and electrospinning and has advantages over electrospinning, such as a higher material production rate, safety, scalability, and low cost [7–9, 21, 22]. The equipment for solution blow spinning consists of a specialized nozzle, a compressed gas, like air or nitrogen, a collector and a pump, to make non-woven webs of polymer micro- and nanofibers, similar to those of the electrospinning technique. As such, the morphologies and properties of the nanofibers produced by the SBS method depend on the process parameters (working distance, spinning gas, pressure, and solution injection rate) and solution variables (solution concentration and viscosity, evaporation rate, surface tension, spinning temperature, and spinning humidity) [21, 22]. The SBS method has been used to produce fibers of several polymers such as polystyrene (PS), poly(methyl methacrylate) (PMMA), poly(lactic acid) (PLA), and poly(ethylene oxide) (PEO) [4, 7–9]. However, to date, the SBS process has rarely been used to prepare nanocomposite fibers [21]. Moreover, the SBS process is considered a new process for the mass production of nanofibers and can be an excellent option to prepare

nanocomposite fibers with morphology and diameters similar to those of the electrospinning process.

In this study, we employed the SBS process for the first time for spinning PLA/TiO<sub>2</sub> anatase solutions with 0, 2.9, 4.8, 9.1, and 16.7 wt% TiO<sub>2</sub>. This load may be important to modify the fiber degradation behavior under UV light, but this study needs to be performed taking into account the process influence, i.e., the SBS process. The results show that this process can be effectively used to produce biodegradable nanocomposite fibers with homogeneous morphology and good properties, indicating that this method can enhance the dispersion of the nanoparticles on the nanofibers.

## Experimental

### Materials

Poly(lactic acid) (PLA,  $M_w = 75,000$  g/mol) pellets were purchased from Biomater Co. (Brazil). TiO<sub>2</sub> anatase with average size of 5 nm was obtained from Aldrich. Chloroform and acetone were purchased from Synth (Brazil) and used as solvents.

### Preparation of PLA/TiO<sub>2</sub> nanocomposites by solution blow spinning

PLA pellets were dissolved in chloroform:acetone at 3:1 (v/v) under vigorous stirring for 2 h at room temperature. The solution was mixed with TiO<sub>2</sub> anatase via ultrasonic dispersion for 10 min, to separate the TiO<sub>2</sub> aggregates. Thus, PLA (6 wt%)/TiO<sub>2</sub> composites were obtained with TiO<sub>2</sub> content of 2.9, 4.8, 9.1, and 16.7 wt% (wt. TiO<sub>2</sub>/wt. PLA). The viscosities of the PLA and PLA/TiO<sub>2</sub> solutions were measured using a Brookfield Viscometer at 10 rpm and at 25 °C. All viscosity measurements were performed in duplicate and values expressed as the mean, as shown in Table 1.

The SBS equipment was home-made, consisting of a syringe pump (KD Scientific, Model 781100) connected to a pressurized air line, a central nozzle with a concentric outer nozzle and an inner nozzle [7, 8]. The inner nozzle was positioned 2 mm beyond the outer nozzle and the working distance was 12 cm. The injection rate was 7.2 ml h<sup>-1</sup> and the air pressure, 60 psi. The nanofibers were collected on a rotating drum (180 rpm), which was wrapped with aluminum foil. Detailed information about the spinning method is available in the literature [7, 8].

**Table 1** Viscosity of PLA/TiO<sub>2</sub> solutions

TiO <sub>2</sub> loading (wt. TiO <sub>2</sub> /wt. PVA)	Viscosity (mPa s)
0.0	19.8
2.9	28.8
4.8	41.7
9.1	60.9
16.7	27.6

## Characterization of the nanocomposites

Fiber morphology was examined using a JEOL model JSM-6510/GS scanning electron microscope (SEM). The fiber diameter was measured using the ImageJ software [23]. For each sample, the average fiber diameter (AFD) and its standard deviation (SD) were determined using SEM images by direct random measurement of at least 100 fibers. An energy dispersive spectrometry (EDS) map was collected using a JEOL model JSM-6510/GS scanning electron microscope filtered with an EDS detector. Transmission electron microscope (TEM) images of the PLA/TiO<sub>2</sub> (4.8 wt%) and PLA/TiO<sub>2</sub> (16.7 wt%) nanofibers were obtained using a Philips CM 120 electron microscope, with an acceleration voltage of 120 kV. The samples were redispersed in isopropanol and two drops of the suspension were deposited on a copper-carbon grid.

The nanocomposite fiber crystal structures were examined by X-ray diffractometry (Shimadzu XRD 6000), with a Ni-filtered CuK $\alpha$  radiation. Scans were carried out from 5° to 50° (2 $\theta$ ) at 0.5°/min. The crystallite sizes of the PLA and TiO<sub>2</sub> nanoparticles were estimated by the Scherrer equation [4].

Thermogravimetric analysis (TGA) was performed using a Q500 TA Instrument. The nanocomposite fibers were analyzed by heating them from 30 to 800 °C at 10 °C/min under nitrogen flow (40 mL min<sup>-1</sup>). Differential scanning calorimetry (DSC) was performed using a Q100 TA Instrument under nitrogen flow at 50 mL min<sup>-1</sup>. The DSC curves were recorded between 25 and 200 °C at a heating rate of 10 °C min<sup>-1</sup>.

The catalytic action associated with anatase TiO<sub>2</sub> nanoparticles in the nanocomposite fibers was evaluated by photocatalytic degradation of Rhodamine (RhB) (Aldrich). This was carried out in a box reactor with six UV-C lamps (100–280 nm). The experiment was performed using about 1 cm<sup>2</sup> of each mat, with TiO<sub>2</sub> equivalent to 0.0035 g in the nanofibers. The samples were introduced into a beaker containing 2.5 mg L<sup>-1</sup> of Rhodamine B solution (20 mL), proceeding to UV irradiation for different time intervals. Furthermore, 0.0035 g of bare TiO<sub>2</sub> was dispersed in the Rhodamine B solution (2.5 mg L<sup>-1</sup>, 20 mL). For comparison, an experiment was performed in the absence of TiO<sub>2</sub> to determine the direct photolysis (self-sensitization) of Rhodamine B.

To evaluate the UV resistance of nanocomposites, a degradation experiment was carried out in the same box reactor as above. The distance between the lamp and the samples was 12 cm and the temperature was about 25 °C. The samples were cut as a rectangular mat, weighing about 6.0 mg. This experiment was conducted for 22 h and the weight loss of PLA by photocatalytic degradation as a function of irradiation time was observed.

## Results and discussion

Figures 1a–c and 2a–c show the SEM images of solution blow spun nanofibers obtained from PLA containing 0, 2.9, 4.8, 9.1, and 16.7 wt% of anatase TiO<sub>2</sub>. Nanofibers with uniform morphology and without beads were produced by the SBS

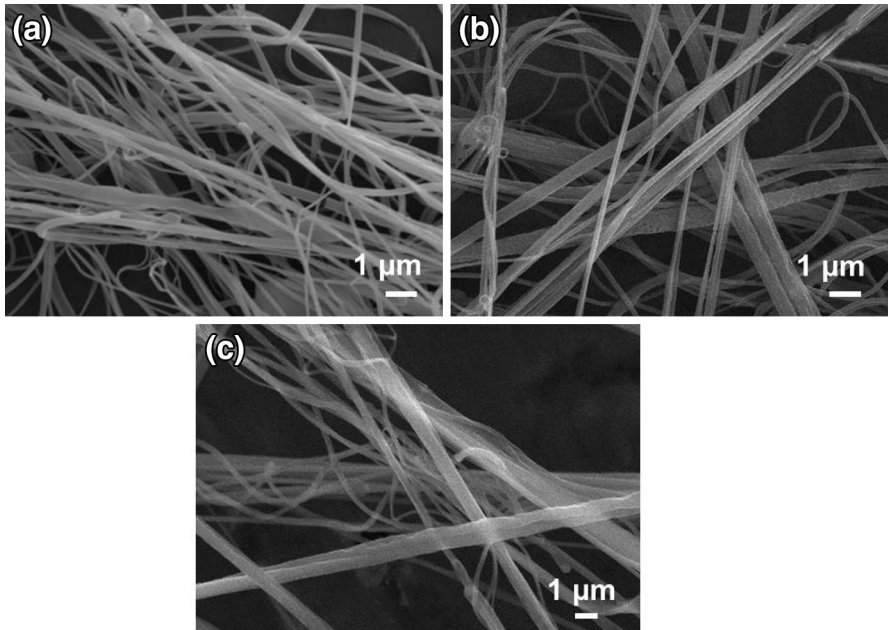


**Fig. 1** SEM images of nanofibers: **a** PLA, **b** PLA/TiO<sub>2</sub> (2.9 wt%), **c** PLA/TiO<sub>2</sub> (4.8 wt%)

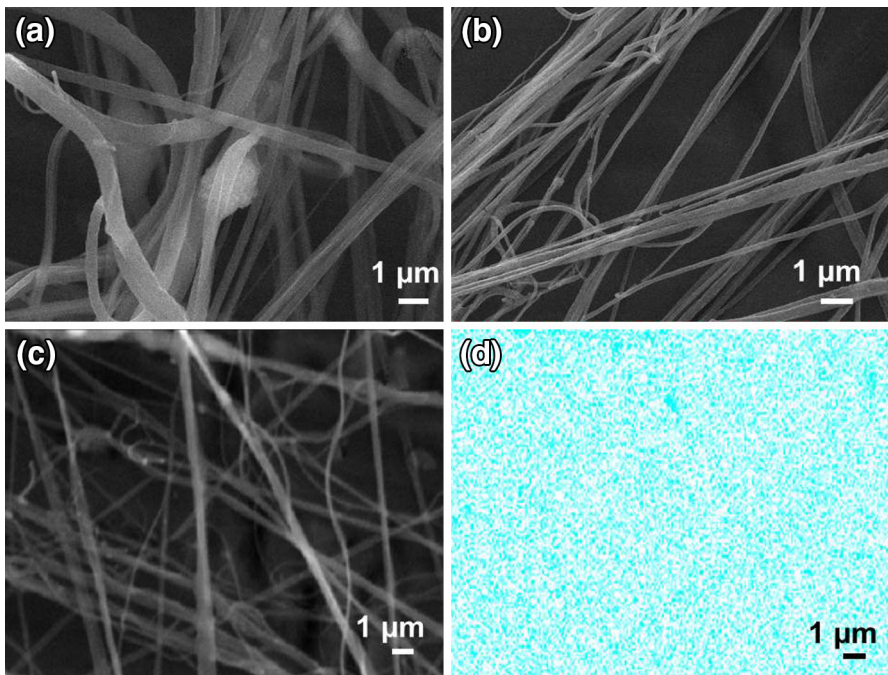


**Fig. 2** SEM images of nanofibers: **a** PLA/TiO<sub>2</sub> (9.1 wt%), **b** PLA/TiO<sub>2</sub> (16.7 wt%). SEM image of **c** PLA/TiO<sub>2</sub> (16.7 wt%) for EDS map of TiO<sub>2</sub>, **d** EDS map of TiO<sub>2</sub>

process. It can be seen that PLA and PLA/TiO<sub>2</sub> fibers have smooth surfaces and no TiO<sub>2</sub> aggregates were observed on the fiber surface. This indicated that TiO<sub>2</sub> nanoparticles were dispersed homogeneously via ultrasound in the PLA solutions and in the spun nanofibers. This result is very important because TiO<sub>2</sub> is a hydrophilic material, whereas PLA is hydrophobic, i.e., spontaneous compatibility is not expected. That implies, therefore, that the PLA viscosity maintained the nanoparticles in suspension, indicating that the SBS process was effective in spinning the fibers in this metastable condition without TiO<sub>2</sub> segregation. This result also agrees with the viscosity measurements of the PLA solutions (Table 1), where a slight increase in viscosity is shown according to the TiO<sub>2</sub> content. The increase is expected for suspensions with a low amount of dispersed, homogeneous particles, and the reduction observed for the sample with 16.7 % TiO<sub>2</sub> is an indication of particle agglomeration. This is reasonable since the high amount of hydrophilic material would lead to phase segregation or precipitation.

The EDS map of a selected region of PLA/TiO<sub>2</sub> (16.7 wt%) fiber is shown in Fig. 2d, where it can be seen that the distribution of the Ti element (in this case, TiO<sub>2</sub> nanoparticles) is uniform, indicating that the SBS process enhanced dispersion of a higher loading of TiO<sub>2</sub> nanoparticles on the fibers. The fiber diameter is presented in Table 2, where we can observe that the average diameters were similar, ranging from 174 ± 56 nm for PLA fibers to 344 ± 155 nm for PLA/TiO<sub>2</sub> (9.1 wt%) fibers, suggesting that the nanoparticle loadings do not significantly affect the final fiber sizes. These results corroborate with the TEM bright-field images of PLA/TiO<sub>2</sub> (Fig. 3), where it is observed that the nanocomposite fibers loaded with 4.8 and 16.7 wt% of TiO<sub>2</sub> have good nanoparticle distribution with some small agglomerates whose average value is 115 nm. However, the dispersion is regular and the nanoparticles are localized without preference on the surface of the fiber or on the bulk. These results agree with the SEM images (Figs. 1, 2), and indicate that the conditions used in the SBS process were successful to tailor the desired uniform nanocomposite fibers.

The X-ray diffraction patterns of the PLA and PLA/TiO<sub>2</sub> fibers obtained by the SBS process are shown in Fig. 4A. The PLA fiber exhibits a peak at  $2\theta = 16.5^\circ$  ascribed to the  $\alpha$  crystals [8]. For all PLA/TiO<sub>2</sub> nanocomposite fibers there is a PLA peak associated with  $\beta$  crystals at  $2\theta = 24^\circ$  and the major peak of anatase TiO<sub>2</sub> at  $2\theta = 25.4^\circ$  [2, 12, 13]. For comparison, the PLA and PLA/TiO<sub>2</sub> films prepared by casting were evaluated by XRD to determine the influence of the SBS method on the polymer crystallization (Fig. 4B). The pattern of PLA and PLA/TiO<sub>2</sub> (9.1 wt%) films reveals four polymer reflection peaks (near 13.9, 16.5, 18.7°), ascribed to the  $\alpha$

**Table 2** Average diameter of solution blow spun nanocomposite fibers

Nanocomposite fibers	Average diameter (nm)
PLA	174 ± 56
PLA/TiO <sub>2</sub> (2.9 wt%)	196 ± 115
PLA/TiO <sub>2</sub> (4.8 wt%)	297 ± 143
PLA/TiO <sub>2</sub> (9.1 wt%)	344 ± 155
PLA/TiO <sub>2</sub> (16.7 wt%)	198 ± 67

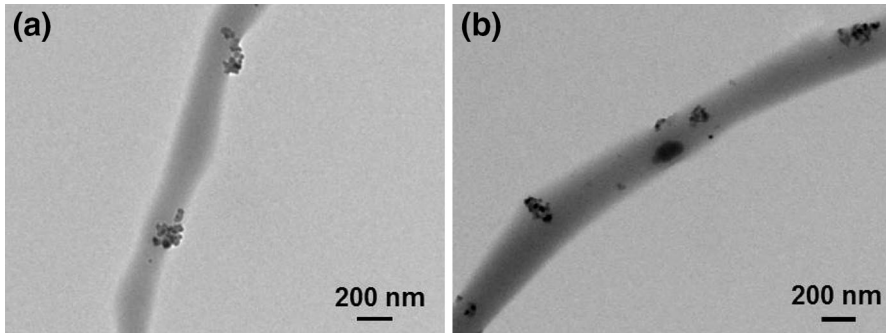


**Fig. 3** TEM bright-field image of nanofibers: **a** PLA/TiO<sub>2</sub> (4.8 wt%), **b** PLA/TiO<sub>2</sub> (16.7 wt%)

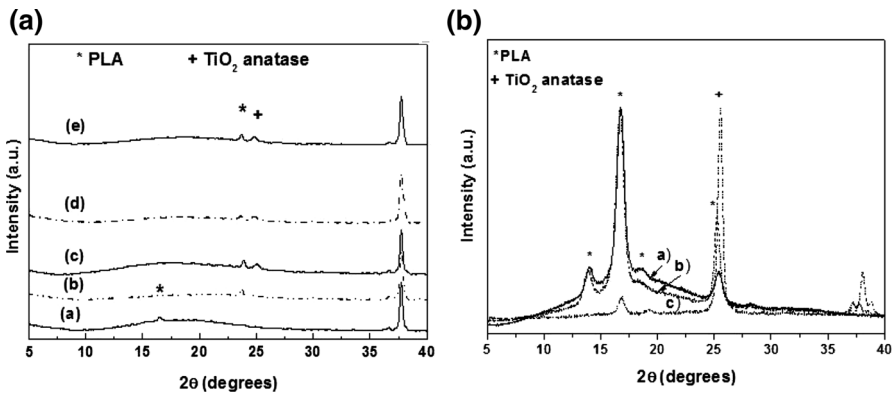


**Fig. 4** X-ray diffraction patterns: **A** nanofibers: *a* PLA, *b* PLA/TiO<sub>2</sub> (2.9 wt%), *c* PLA/TiO<sub>2</sub> (4.8 wt%), *d* PLA/TiO<sub>2</sub> (9.1 wt%), and *e* PLA/TiO<sub>2</sub> (16.7 wt%). **B** Nanocomposite films prepared by casting: *a* PLA, *b* PLA/TiO<sub>2</sub> (9.1 wt%), and *c* PLA/TiO<sub>2</sub> (16.7 wt%)

phase, and a peak (near 25°) associated with the  $\beta$  phase [8]. However, the pattern of the PLA/TiO<sub>2</sub> (16.7 wt%) film has no peak at 13.9° and has a strong peak at 25.5° (TiO<sub>2</sub> anatase) [12, 13]. When PLA fibers are compared with PLA films prepared by casting, we can clearly see that films have preferential crystallization at 16.5° ( $\alpha$  crystals), which is not affected significantly by the higher TiO<sub>2</sub> loading (16.7 wt%) on the PLA film and these nanoparticles only decrease the intensities of the PLA peaks. These results show that TiO<sub>2</sub> nanoparticles do not impede the crystallization path of the PLA phase and the SBS method preferentially induces the formation of crystals at 25° ( $\beta$  phase) probably because of the different deformation extent of the molecules during the fiber formation process. The casting method has a lower solvent evaporation rate resulting in higher amounts of PLA crystals.

To characterize the thermal behavior of PLA nanofibers, PLA films prepared by casting and their PLA/TiO<sub>2</sub> nanocomposites, TG, DTG, and DSC analyses were carried out (Figs. 5, 6, 7, 8). The TG curves show that for PLA/TiO<sub>2</sub> fibers and films, the final residue of the nanocomposites increases as the TiO<sub>2</sub> content increase

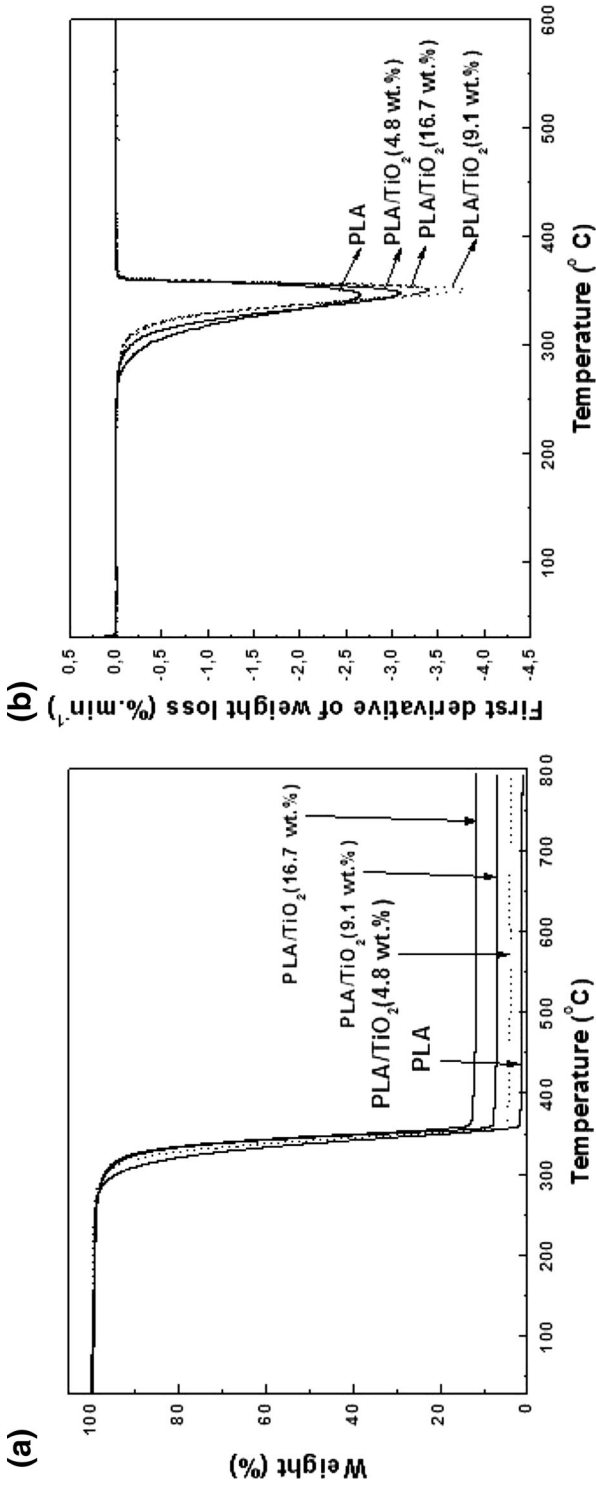


**Fig. 5** a Thermogravimetric curves and b DTG nanofiber curves: PLA, PLA/TiO<sub>2</sub> (4.8 wt%), PLA/TiO<sub>2</sub> (9.1 wt%), and PLA/TiO<sub>2</sub> (16.7 wt%)



**Fig. 6** DSC nanofiber thermograms: *a* PLA, *b* PLA/TiO<sub>2</sub> (4.8 wt%), *c* PLA/TiO<sub>2</sub> (9.1 wt%), and *d* PLA/TiO<sub>2</sub> (16.7 wt%)

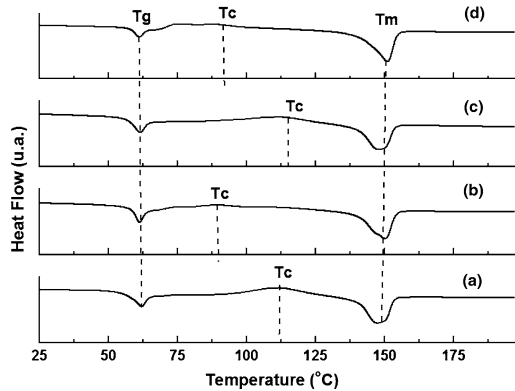


(Table 3), indicating that the TiO<sub>2</sub> is well dispersed along the fibers. Since TG is an analytical technique that is sensitive to the real TiO<sub>2</sub> contents, we observed that, in the cases where the material was poorly dispersed, phase separation took place, which implicate in lower effective TiO<sub>2</sub> contents on the final material—but only observed by TG analysis. In our samples, the good dispersion permits that, during the spinning process, the precursor solution maintains the same TiO<sub>2</sub> content along the process, which results in the final material having loading amounts equivalent to the expected.

DTG curves for the samples (Figs. 5b, 7b) corroborate these results, which show one weight loss step during degradation around 265–365 °C. However, there is a slight weight loss around 80–135 °C for PLA and PLA/TiO<sub>2</sub> films obtained by casting, which can be attributed to the solvent residue (chloroform:acetone). This behavior was not observed for solution blow spun nanofibers because of the high solvent evaporation rate during this process [7, 8].

The DSC curves (Figs. 6, 8) were used to determine characteristic temperatures, glass transition temperature ( $T_g$ ), crystallization temperature ( $T_c$ ), melting temperature ( $T_m$ ), heat of crystallization ( $\Delta H_c$ ), and heat of fusion ( $\Delta H_f$ ) for all the samples as shown in Table 3. It was observed that the thermal behavior of nanocomposites produced by the SBS technique and the casting method were similar. The intense melting peak ( $T_m$ ) at around 146–151 °C for all the samples had high values of  $\Delta H_f$  (21–29 J/g) (Table 3). The exothermic peaks ( $T_c$ ) near 110 °C are associated with the PLA crystallization, whose lower  $\Delta H_c$  values (0.9–14 J/g) confirm the semicrystalline nature of the polymer. However, the  $T_c$  peak was not observed for PLA/TiO<sub>2</sub> (16.7 wt%) cast film (Fig. 8c) because it was the sample with the highest percentage of TiO<sub>2</sub> (almost 15 % TiO<sub>2</sub>, taking in account the PLA residue). In this case, the TiO<sub>2</sub> nanoparticles could be nucleating agents for the polymer crystallization. The DSC curve of PLA/TiO<sub>2</sub> (16.7 wt%) cast film corroborate with their X-ray diffraction pattern (Fig. 4B), where it is clear that the PLA crystallization decreases.

To evaluate the surface accessibility of TiO<sub>2</sub> nanoparticles dispersed in the solution blow spun nanofibers, a catalytic experiment using a dye was performed.

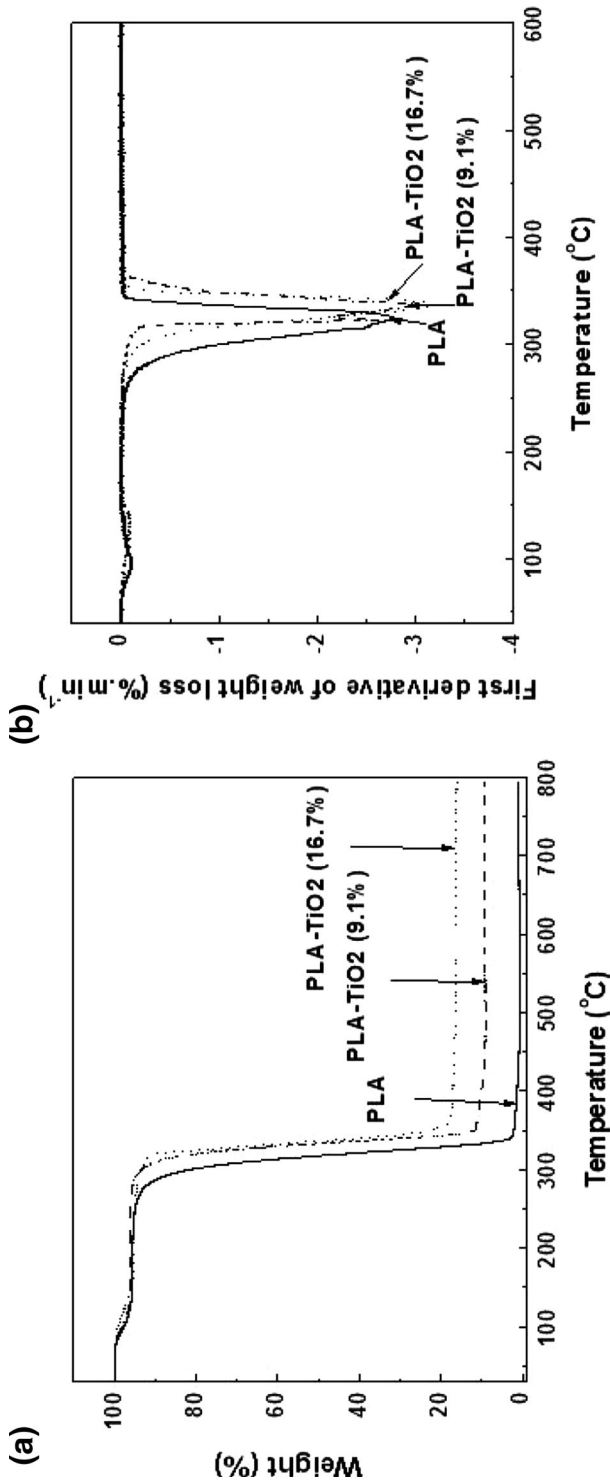


**Fig. 7** a Thermogravimetric curves and b DTG curves of nanocomposites prepared by casting: PLA, PLA/TiO<sub>2</sub> (9.1 wt%), and PLA/TiO<sub>2</sub> (16.7 wt%)

**Fig. 8** DSC thermograms of nanocomposites prepared by casting: *a* PLA, *b* PLA/TiO<sub>2</sub> (9.1 wt%), and *c* PLA/TiO<sub>2</sub> (16.7 wt%)

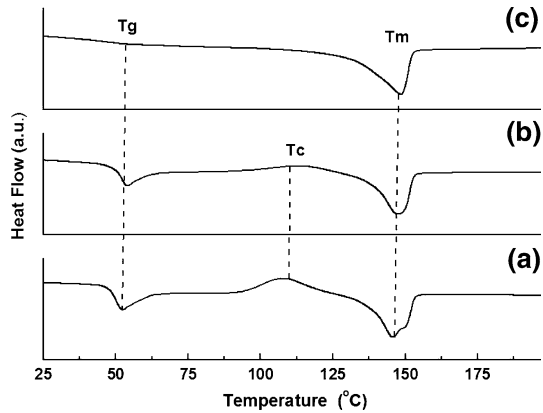


**Table 3** Percentage of residue ( $T_g$  data) and DSC data [characteristic temperatures, heat crystallization ( $\Delta H_c$ ), heat fusion ( $\Delta H_f$ )] for PLA fiber, PLA film, and its nanocomposites with TiO<sub>2</sub>

Sample	% Residue	$T_g$ (°C)	$T_c$ (°C)	$T_m$ (°C)	$\Delta H_c$ (J/g)	$\Delta H_f$ (J/g)
PLA fiber	1.2	62	111	147	14	26
PLA/TiO <sub>2</sub> (4.8 wt%) fiber	3.9	61	90	150	2.5	28
PLA/TiO <sub>2</sub> (9.1 wt%) fiber	6.8	61	112	148	5.4	25
PLA/TiO <sub>2</sub> (16.7 wt%) fiber	11.7	61	90	151	0.9	27
PLA film	1.1	53	109	146	11	23
PLA/TiO <sub>2</sub> (9.1 wt%) film	9.3	54	113	148	4.9	21
PLA/TiO <sub>2</sub> (16.7 wt%) film	16.1	55	–	149	–	29

The values of  $(C \cdot Co^{-1}) \times 100 \%$  obtained from Rhodamine B photodegradation curves under UV-C light radiation with different samples and various conditions are shown in Fig. 9a where a column graph represents the  $(C \cdot Co^{-1}) \times 100 \%$  values. It can be seen that the degradation of the dye with all the PLA/TiO<sub>2</sub> fibers is slightly greater than the self-sensitization of RhB after 6 h, showing that the SBS nanofibers have some photocatalytic activity, as expected. This suggests the presence of some nanoparticles at the surface of the polymer. When comparing equivalent amounts of anatase TiO<sub>2</sub>, it is observed that after 0.5 and 6 h, the percentage values of  $C \cdot Co^{-1}$  of dye degradation with all the PLA/TiO<sub>2</sub> fibers are much lower than with the nanopowder of anatase TiO<sub>2</sub>. However, the values of  $(C \cdot Co^{-1}) \times 100 \%$  photodegradation of RhB of each fiber is almost the same (about 64 % in 6 h). This result also indicates that part of the TiO<sub>2</sub> nanoparticles in the nanocomposite is not accessible to the dye solution. Moreover, small nanoparticle agglomerates that were observed by TEM bright-field images in nanofibers (Fig. 3) could contribute to the decrease in the photodegradation of RhB.

Figure 9b shows the weight loss of PLA fiber and PLA/TiO<sub>2</sub> nanocomposite fibers along with irradiation time in air. It can be seen that the weight loss percent of

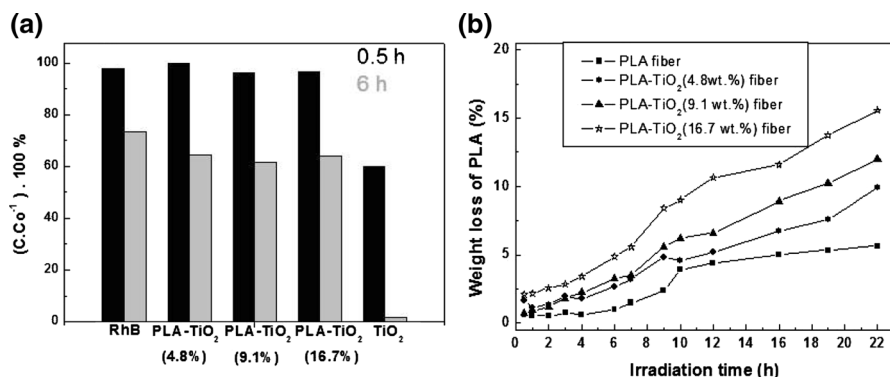


**Fig. 9** **a** Column graph of  $(C-Co^{-1}) \times 100 \%$  values under UV-C illumination for Rhodamine-B solution using PLA/TiO<sub>2</sub> (4.8 wt%) fiber, PLA/TiO<sub>2</sub> (9.1 wt%) fiber, PLA/TiO<sub>2</sub> (16.7 wt%) fiber, and bare TiO<sub>2</sub> (anatase). **b** Weight loss of PLA: PLA fiber, PLA/TiO<sub>2</sub> (4.8 wt%) fiber, PLA/TiO<sub>2</sub> (9.1 wt%) fiber, and PLA/TiO<sub>2</sub> (16.7 wt%) fiber under UV-C light against irradiation time in air

PLA in all the PLA/TiO<sub>2</sub> samples increases with the increase in TiO<sub>2</sub> content after 22 h, about 16 % for PLA/TiO<sub>2</sub> (16.7 wt%) and 10 % for PLA/TiO<sub>2</sub> (4.8 wt%). This indicates that the TiO<sub>2</sub> nanoparticles are well distributed on the polymer nanofiber.

## Conclusion

These results show that the SBS process is effective for producing nanocomposites even in cases where the loading material is poorly compatible with the matrix, as in TiO<sub>2</sub> and PLA. Despite deviations in the total loading compared to the initial amount added, the final fibers were homogeneous, showing low TiO<sub>2</sub> agglomeration even at higher TiO<sub>2</sub> loading.

The X-ray diffraction patterns of the PLA/TiO<sub>2</sub> nanocomposites show that TiO<sub>2</sub> nanoparticles do not impede the crystallization path of the polymer by the SBS method and casting method. However, these results show that the SBS method preferentially induces the formation of crystals at 25° ( $\beta$  phase). The TGA analysis reveals that for PLA/TiO<sub>2</sub> nanocomposites, the final residue increases as the TiO<sub>2</sub> content increases, confirming that the TiO<sub>2</sub> dispersion was a success. Differential scanning calorimetry (DSC) results demonstrate that the thermal behavior of nanocomposites produced by the SBS technique and the casting method are similar.

The nanoparticles are active for dye degradation, but this effect was associated with a smaller amount on the fiber surfaces. On the other hand, their effect on the fiber photodegradation is remarkable, increasing the PLA photodegradation rate threefold at higher TiO<sub>2</sub> loadings. These findings are useful to understand the method capabilities, as well as to determine optimal conditions for TiO<sub>2</sub> dispersion in the material seeking improvement in biodegradation behaviors.

**Acknowledgments** The authors are grateful for financial support from CAPES, CNPq (Process No. 301173/2013-3) and FAPESP.

## References

1. Man C, Zhang C, Liu Y, Wang W, Ren W, Jiang L, Reisdorffer F, Nguyen TP, Dan Y (2012) Poly (lactic acid)/titanium dioxide composites: preparation and performance under ultraviolet irradiation. *Polym Degrad Stabil* 97:856–862
2. Buzarovska A, Grozdanov A (2012) Biodegradable poly(L-lactic acid)/TiO<sub>2</sub> nanocomposites: thermal properties and degradation. *J Appl Polym Sci* 123:2187–2193
3. Chen C, Pan C, Song M, Wu C, Guo D, Wang X, Chen B, Gu Z (2007) Poly(lactic acid) PLA based nanocomposites—a novel way of drug-releasing. *Biomed Mater* 2:L1–L4
4. Oliveira JE, Moraes EA, Marconcini JM, Mattoso LHC, Glenn GM, Medeiros ES (2013) Properties of poly(lactic acid) and poly(ethylene oxide) solvent polymer mixtures and nanofibers made by solution blow spinning. *J Appl Polym Sci* 129:3672–3681
5. Costa RGF, Oliveira JE, Paula GF, Picciani PHS, Medeiros ES, Ribeiro C, Mattoso LHC (2012) Eletrofição de polímeros em solução: parte I: fundamentação teórica. *Polímeros* 22:170–177
6. Costa RGF, Oliveira JE, Paula GF, Picciani PHS, Medeiros ES, Ribeiro C, Mattoso LHC (2012) Eletrofição de polímeros em solução: parte II: aplicações e perspectivas. *Polímeros* 22:178–185
7. Oliveira JE, Moraes EA, Costa RGF, Afonso AS, Mattoso LHC, Orts WJ, Medeiros ES (2011) Nano and submicrometric fibers of poly(D, L-lactide) obtained by solution blow spinning: process and solution variables. *J Appl Polym Sci* 122:3396–3405
8. Oliveira JE, Medeiros ES, Cardozo L, Voll F, Madureira EH, Mattoso LHC, Assis OBG (2013) Development of poly(lactic acid) nanostructured membranes for the controlled delivery of progesterone to livestock animals. *Mater Sci Eng C* 33:844–849
9. Medeiros ES, Glenn GM, Klamczynski AP, Orts WJ, Mattoso LHC (2009) Solution blow spinning: a new method to produce micro- and nanofibers from polymer solutions. *J Appl Polym Sci* 113:2322–2330
10. Costa RGF, Ribeiro C, Mattoso LHC (2010) Preparation and characterization of PVA-Ag nanocomposite fibers with antibacterial activities. *Sci Adv Mat* 2:157–162
11. Cargnello M, Gordon TR, Murray CB (2014) Solution-phase synthesis of titanium dioxide nanoparticles and nanocrystals. *Chem Rev* 114:9319–9345
12. Costa RGF, Ribeiro C, Mattoso LHC (2010) Morphological and photocatalytic properties of PVA/TiO<sub>2</sub> nanocomposite fibers produced by electrospinning. *J Nanosci Nanotechnol* 10:5144–5152
13. Costa RGF, Ribeiro C, Mattoso LHC (2013) Study of the effect of rutile/anatase TiO<sub>2</sub> nanoparticles synthesized by hydrothermal route in electrospun PVA/TiO<sub>2</sub> nanocomposites. *J Appl Polym Sci* 127:4463–4469
14. Machado AV, Amorim S, Botelho G, Neves IC, Fonseca AM (2013) Nanocomposites of poly(epsilon-caprolactone) doped with titanium specie. *J Mater Sci* 48:3578–3585
15. Gupta KK, Kundan A, Mishra PK, Srivastava P, Mohanty S, Singh NK, Mishra A, Maiti P (2012) Polycaprolactone composites with TiO<sub>2</sub> for potential nanobiomaterials: tunable properties using different phases. *Phys Chem Chem Phys* 14:12844–12853
16. Prahsarn C, Klinsukhon W, Roungpaisan N (2011) Electrospinning of PAN/DMF/H<sub>2</sub>O containing TiO<sub>2</sub> and photocatalytic activity of their webs. *Mater Lett* 65:2498–2501
17. Zhang J, Ji Q, Shen X, Xia Y, Tan L, Wang F, Kong Q (2012) Flame retardancy and non-isothermal crystallization behaviour of PET/TiO<sub>2</sub> nanocomposites. *Polym Polym Compos* 20:399–405
18. Buzarovska A (2013) PLA nanocomposites with functionalized TiO<sub>2</sub> nanoparticles. *Polym Plast Technol Eng* 52:280–286
19. Farhoodi M, Dadashi S, Mousavi SMA, Rahmat SG, Djomeh ZA, Oromiehie A, Hemmati F (2012) Influence of TiO<sub>2</sub> nanoparticle filler on the properties of PET and PLA nanocomposites. *Polymer (Korea)* 36:745–755
20. Song M, Pan C, Chen C, Li J, Wang X, Gu Z (2008) The application of new nanocomposites: enhancement effect of polylactide nanofibers/nano-TiO<sub>2</sub> blends on biorecognition of anticancer drug daunorubicin. *Appl Surf Sci* 255:610–612
21. Oliveira JE, Zucolotto V, Mattoso LHC, Medeiros ES (2011) Multi-wall carbon nanotube/poly(lactic acid) nanocomposite fibrous membranes prepared by Solution Blow Spinning. *J Nanosci Nanotechnol* 11:1–9
22. Medeiros ES, Glenn GM, Klamczynski AP, Orts WJ, Mattoso LHC (2009) Solution blow spinning, U.S. Patent No. 61/249
23. Software ImageJ. <http://rsbweb.nih.gov/ij/index.html>. Accessed 2 Dec 2014